Calcium flux in monocytes. Elutriated human monocytes ($10^7 ml^{-1}$) were loaded with $1.0 \mu M$ Fura-2 AM (Molecular Probes) in the dark for 15 min at $37 °C$ in DPBS containing 0.1% HSA, and intracellular calcium was measured as described[28]. The data are presented as the relative ratio of fluorescence at 340 and 380 nm.

Chemotaxis assays. Chemotaxis assays were carried out in a 48-well micro-chemotaxis chamber (NeuroProbe) at $37 °C$ for 90 min[29] on elutriated mono-cytes in HBSS buffer (MediaTech) supplemented with 0.05% low endotoxin BSA (Sigma) at 5×10^6 cells ml^{-1}. Monocytes that migrated across the filter and adhered to the bottom side were stained with Diff-Quick (Baxter Scientific). The cells per three 400× fields in duplicate wells were counted and the data expressed as the mean ± standard deviation.

Statistical analysis. Data are expressed as the mean ± standard deviation or standard error of the mean, as indicated. Statistical comparison of means was performed by two-tailed unpaired Student's t-test. The null hypothesis was considered to be rejected at $P < 0.05$.

1. Smith, J. D. *et al.* Decreased atherosclerosis in mice deficient in both macrophage colony-stimulating factor (op) and apolipoprotein E. *Proc. Natl Acad. Sci. USA* **92,** 8264–8268 (1995).
2. Suzuki, H. *et al.* A role for macrophage scavenger receptors in atherosclerosis and susceptibility to infection. *Nature* **386,** 292–296 (1997).
3. Fazio, S. *et al.* Increased atherosclerosis in mice reconstituted with apolipoprotein E null macro-phages. *Proc. Natl Acad. Sci. USA* **94,** 4647–4652 (1997).
4. Nelken, N. A., Coughlin, S. R., Gordon, D. & Wilcox, J. N. Monocyte chemoattractant protein-1 in human atheromatous plaques. *J. Clin. Invest.* **88,** 1121–1127 (1991).
5. Koch, A. E. *et al.* Enhanced production of the chemotactic cytokines interleukin-8 and monocyte chemoattractant protein-1 in human abdominal aortic aneurysms. *Am. J. Pathol.* **142,** 1423–1431 (1993).
6. Boisvert, W. A., Santiago, R., Curtiss, L. K. & Terkeltaub, R. A. A leukocyte homologue of the IL-8 receptor CXCR-2 mediates the accumulation of macrophages in atherosclerotic lesions of LDL receptor-deficient mice. *J. Clin. Invest.* **101,** 353–363 (1998).
7. Boring, L., Goslin, J., Cleary, M. & Charo, I. Decreased lesion formation in CCR2-/- mice reveals a role for chemokines in the initiation of atherosclerosis. *Nature* **394,** 894–897 (1998).
8. Baggiolini, M., Dewald, B. & Moser, B. Interleukin-8 and related chemokines—CXC and CC chemokines. *Adv. Immunol.* **55,** 97–179 (1994).
9. Gersten, R. E. *et al.* Adhesion of monocytes to vascular cell adhesion molecule-1-transduced human endothelial cells: implications for atherogenesis. *Circ. Res.* **82,** 871–878 (1998).
10. Berkhout, T. A. *et al.* Cloning, *in vitro* expression, and functional characterization of a novel human CC chemokine of the monocyte chemoattractant protein (MCP) family that binds and signals through the CC chemokine receptor 2B. *J. Biol. Chem.* **272,** 16404–16413 (1997).
11. Springer, T. A. Traffic signals for lymphocyte recirculation and leukocyte emigration: the multistep paradigm. *Cell* **76,** 301–314 (1994).
12. Weber, C., Alon, R., Moser, B. & Springer, T. A. Sequential regulation of alpha 4 beta 1 and alpha 5 beta 1 integrin avidity by CC chemokines in monocytes: implications for transendothelial chemotaxis. *J. Cell Biol.* **134,** 1063–1073 (1996).
13. Woldemar-Carr, M., Alon, R. & Springer, T. A. The C-C chemokine MCP-1 differentially modulates the avidity of β1 and β2 integrins on T lymphocytes. *Immunity* **4,** 179–187 (1996).
14. Yoshimura, T. *et al.* Purification of a human monocyte-derived neutrophil chemotactic factor that has peptide sequence similarity to other host defense cytokines. *Proc. Natl Acad. Sci. USA* **84,** 9233–9237 (1987).
15. Schroder, J. M., Mrowietz, U., Morita, E. & Christophers, E. Purification and partial biochemical characterization of a human monocyte-derived, neutrophil-activating peptide that lacks interleukin 1 activity. *J. Immunol.* **139,** 3474–3483 (1987).
16. Chuntharapai, A., Lee, J., Hebert, C. A. & Kim, K. J. Monoclonal antibodies detect different distribution patterns of IL-8 receptor A and IL-8 receptor B on human peripheral blood leukocytes. *J. Immunol.* **153,** 5682–5688 (1994).
17. Premack, B. A. & Schall, T. J. Chemokine receptors: gateways to inflammation and infection. *Nat. Med.* **2,** 1174–1178 (1996).
18. Jones, K. A. *et al.* GABA(B) receptors function as a heteromeric assembly of the subunits GABA(B)R1 and GABA(B)R2. *Nature* **396,** 674–679 (1998).
19. Luscinskas, F. W. *et al.* Monocyte rolling, arrest and spreading on IL-4-activated vascular endothelium under flow is mediated via sequential action of L-selectin, beta 1-integrins, and beta 2-integrins. *J. Cell Biol.* **125,** 1417–1427 (1994).
20. Gersten, R. *et al.* Adhesion of memory lymphocytes to VCAM-1-transduced human vascular endothelial cells under simulated physiological flow conditions *in vitro. Circ. Res.* **79,** 1205–1215 (1996).
21. Yoshida, M., Szente, B. E., Kiely, J.-M., Rosenzweig, A. & Gimbrone, M. A. Regulation of E-selectin phosphorylation during leukocyte adhesion: a novel outside-in signaling role for E-selectin. *J. Immunol.* **161,** 933–941 (1997).
22. Graber, N. *et al.* T cells bind to cytokine-activated endothelial cells via a novel, inducible sialoglycoprotein and endothelial leukocyte adhesion molecule-1. *J. Immunol.* **145,** 819–830 (1990).
23. Bevilacqua, M. P., Prober, J. S., Mendrick, D. L., Cotran, R. S. & Gimbrone, M. A. Identification of an inducible endothelial-leukocyte adhesion molecule. *Proc. Natl Acad. Sci. USA* **84,** 9238–9242 (1987).
24. Luscinskas, F. W. *et al.* Cytokine-activated human endothelial monolayers support enhanced neutrophil transmigration via a mechanism involving both endothelial-leukocyte adhesion mole-cule-1 and intercellular adhesion molecule-1. *J. Immunol.* **146,** 1617–1625 (1991).
25. Taichman, D. B. *et al.* Tumor cell surface alpha 4 beta 1 integrin mediates adhesion to vascular endothelium: demonstration of an interaction with the N-terminal domains of INCAM-110/VCAM-1. *Cell Regul.* **2,** 347–355 (1991).
26. Luscinskas, F. W. *et al.* L- and P-selectins, but not CD49d (VLA4) integrins, mediate monocyte initial attachment to TNF-activated vascular endothelium *in vitro. J. Immunol.* **156,** 326–335 (1996).
27. Shen, J., Luscinskas, F. W., Connolly, A., Dewey, C. F. J. & Gimbrone, M. A. Fluid shear stress modulates cytosolic free calcium in vascular endothelial cells. *Am. J. Physiol.* **262,** C384–390 (1992).
28. Wheeler, M. E., Luscinskas, F. W., Bevilacqua, M. P. & Gimbrone, M. A. Cultured human endothelial cells stimulated with cytokines or endotoxin produce an inhibitor of leukocyte adhesion. *J. Clin. Invest.* **82,** 1211–1218 (1988).
29. Falk, W., Goodwin, R. H. Jr & Leonard, E. J. A 48-well micro chemotaxis assembly for rapid and accurate measurement of leukocyte migration. *J. Immunol. Meth.* **33,** 239–247 (1980).

Tyro-3 family receptors are essential regulators of mammalian spermatogenesis

Qingxian Lu*†, Martin Gore*†‡, Qing Zhang§,
Todd Camenisch‖, Sharon Boast§, Franca Casagranda¶,
Cary Lai#, Michael K. Skinner☆, Rüdiger Klein¶,
Glenn K. Matsushima‖, H. Shelton Earp**, Stephen P. Goff§
& Greg Lemke*

* *Molecular Neurobiology Laboratory, Salk Institute for Biological Studies, La Jolla, California 92037, USA*
§ *Howard Hughes Medical Institute and Department of Biochemsitry & Molecular Biophysics, Columbia University College of Physicians and Surgeons, New York, New York 10032, USA*
‖ *Neuroscience Center and Department of Microbiology & Immunology, and*
** *Lineberger Comprehensive Cancer Center, University of North Carolina, Chapel Hil, North Carolina 27599, USA*
¶ *Developmental Biology Programme, European Molecular Biology Laboratory, 69117 Heidelberg, Germany*
# *Department of Neuropharmacology, Scripps Research Institute, La Jolla, California 92037, USA*
☆ *Center for Reproductive Biology, Department of Genetics and Cell Biology, Washington State University, Pullman, Washington 99164, USA*
† *These authors contributed equally to this work.*

..

We have generated and analysed null mutations in the mouse genes encoding three structurally related receptors with tyrosine kinase activity: Tyro 3, Axl, and Mer[1–4]. Mice lacking any single receptor, or any combination of two receptors, are viable and fertile, but male animals that lack all three receptors produce no mature sperm, owing to the progressive death of differentiating germ cells. This degenerative phenotype appears to result from a failure of the tropic support that is normally provided by Sertoli cells of the seminiferous tubules, whose function depends on testosterone and additional factors produced by Leydig cells[5–7]. Tyro 3, Axl and Mer are all normally expressed by Sertoli cells during postnatal development, whereas their ligands, Gas6 and protein S, are produced by Leydig cells before sexual maturity, and by both Leydig and Sertoli cells thereafter. Here we show that the concerted activation of Tyro 3, Axl and Mer in Sertoli cells is critical to the role that these cells play as nurturers of developing germ cells. Additional observations indicate that these receptors may also be essential for the tropic maintenance of diverse cell types in the mature nervous, immune and reproductive systems.

The receptor protein-tyrosine kinases (PTKs) of the mammalian Tyro 3 family[8] include Tyro 3 (also named Rse, Sky, Brt, Tif, Dtk, Etk-2)[2,9,10], Axl (also named Ark, Ufo, Tyro 7)[3,11,12] and Mer (also named Eyk, Nyk, Tyro 12)[4,13]. These three receptors are widely expressed in adult tissues, but their function is unknown. They share a distinctive structure, with extracellular regions composed of two immunoglobulin-related domains linked to two fibronectin type-III repeats, and cytoplasmic regions that contain an intrinsic PTK domain. Tyro 3, Axl and Mer are present in variable amounts in

neural, lymphoid, vascular and reproductive tissues, and in primary and tumour cell lines derived from these sources[1,3,10–13]. The kinase activity of each of the receptors is activated by Gas6 (refs 14–17), a ligand that exhibits sequence relatedness to a steroid hormone transport protein designated the sex-hormone-binding globulin[18]. Tyro 3 can also bind and be activated by protein S, an anticoagulant in the blood coagulation cascade whose structure is closely related to that of Gas6 (ref. 14), although the extent to which protein S functions as a Tyro 3 ligand *in vivo* is debated[15].

We investigated the function of Tyro 3, Axl and Mer by inactivating their genes in the mouse[19] (Fig. 1). Mice homozygous for any single gene mutation were viable and fertile, and displayed no gross anatomical defects. Although activity-induced seizures have been observed in Tyro 3 single mutants more than seven months old (Q.L., M.G. and G.L., data not shown), and there is a two-fold increase in spleen size with an accompanying deficit in monocyte response to endotoxins in Mer homozygotes[20], all single mutants were obtained at the expected Mendelian frequency at weaning, and
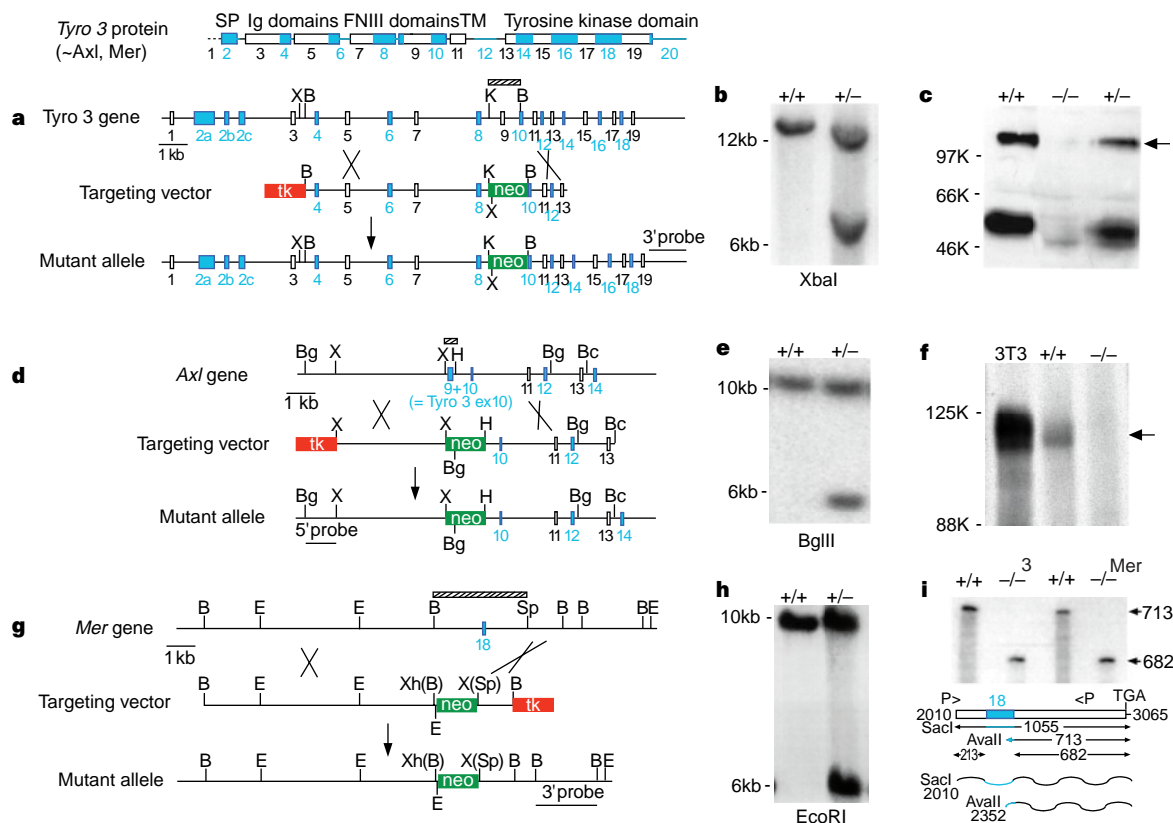
Figure 1 Inactivation of the mouse *Tyro 3*, *Axl* and *Mer* genes. The shared domain structure of these receptors is shown schematically (top); numbers denote exons of the mouse *Tyro 3* gene[27]. **a**, Structure of the mouse *Tyro 3* gene, the targeting vector for inactivation, and the recombined allele. Signal peptide (SP) exons are numbered according to ref. 28, remaining exons are positioned according to ref. 27, with designations one integer lower after exon 3 (for example, exon 7 here is exon 8 of ref. 27). The 3′ probe used for detection of homologous recombination of the right arm of the targeting vector is indicated. Ig, immunoglobulin-like; FNIII, fibronectin type III-like; TM, transmembrane domain; neo, G418 positive selection cassette; tk, thymidine kinase negative selection cassette; B, *Bam*HI; K, *Kpn*I; X, *Xba*I. **b**, Southern blot of *Xba*I-digested DNA from ES cells homozygous (+/+) or heterozygous (+/−) for the normal *Tyro 3* gene, hybridized with the 3′ probe indicated in **a**. **c**, Western blot of brain protein lysates from wild-type (+/+), homozygous mutant (−/−), or heterozygous mutant mice (+/−), probed with a Tyro 3-specific antibody[2]. Tyro 3 is arrowed. **d**, Structure of the *Axl* gene, the targeting vector for inactivation, and the recombined allele. Only the indicated exons have been mapped, although the targeting vector is likely to contain additional exons within its flanking arms, based on the structure of the human *Axl* gene[29]. The 5′ probe used for detection of homologous recombination of the left arm of the targeting vector is indicated. Bg, *Bgl*II; Bc, *Bcl*I; H, *Hin*dIII. **e**, Southern blot of *Bgl*II-digested DNA from ES cells homozygous (+/+) and heterozygous (+/−) for the normal *Axl* gene, hybridized with the 5′ probe indicated in **d**. **f**, Western blot of total brain protein lysates prepared from wild-type (+/+) or homozygous mutant (−/−) mice, immunoprecipitated with an Axl-specific antibody[30] and then probed with the same antibody. NIH3T3 cells, which express high levels of the receptor[30], were similarly analysed as a positive control. Axl is indicated by an arrow. **g**, Restriction map of the mouse *Mer* gene and structure of

the targeting vector for the gene inactivation and of the recombined allele. The *Mer* exon that corresponds to exon 18 of the mouse *Tyro 3* gene (exon 19 of ref. 27) is contained within the indicated 3.1-kb *Bam*HI–*Spe*I (B–Sp) restriction fragment, but its precise location is unknown. Other *Mer* exons have not been mapped. The 53 and 1/3 amino acids of exon 18 extend from Met 725 in kinase sub-domain VI to Val 778 in sub-domain X. The 3′ probe used for detection of homologous recombination of the right arm of the targeting vector is indicated. E, *Eco*RI; Xh, *Xho*I. **h**, Southern blot of *Eco*RI-digested tail DNA from mice homozygous (+/+) and heterozygous (+/−) for the *Mer* gene, hybridized with the 3′ probe indicated in **g**. **i**, RNase protection analysis (RPA) of RNAs isolated from adult wild-type (+/+), Mer single mutant (−/−^Mer), and triple mutant (−/−^3) mouse testes. Two radio-labelled RPA probes (wavy lines) were used: one runs from a *Sac*I site at nucleotide 2010 of the mouse Mer cDNA[4] to nucleotide 3,065 (just downstream of the Mer TGA stop codon), and the second from an *Ava*II site at nucleotide 2,352 to nucleotide 3,065. RPA results using the *Ava*II probe are shown. This probe is fully protected from RNase digestion following hybridization to wild-type RNA (713-bp band), but is trimmed to a 682-bp fragment following hybridization to either Mer single or triple mutant RNA (arrowed lines). Similar RPAs with the *Sac*I probe (gels not shown) yielded the same 682-bp protected fragment upon hybridization to Mer mutant RNA, and also a protected fragment of 213 bp (arrowed). To confirm that these corresponded to deletion of the indicated Mer exon (blue), we performed RT-PCR on Mer mutant RNA using the indicated PCR primers (P> and <P). Sequencing of the amplified product demonstrated that only this exon (equivalent to *Tyro 3* exon 18 in **a**, or exon 19 of ref. 27) is deleted in the mutant. This 160-nucleotide deletion removes residues in kinase subdomains VII–IX, and portions of VI and X, which are essential to the activity of all known tyrosine kinases.

all lived for a long time in the laboratory. These results indicate that no single receptor of the Tyro 3 family is essential during embryonic development.

Because individual members of receptor PTK families often form heterodimers with one another to yield hybrid receptors with overlapping binding specificities, and co-expression of Tyro 3 and Axl or Mer has been observed for several cell types, we generated Tyro 3/Axl and Tyro 3/Mer double mutants. These mice were also obtained in the expected Mendelian ratios (we found that the *Tyro 3* and *Mer* genes are linked in the mouse genome) and were also viable and superficially healthy (but see below). Many double mutants, both male and female, were fertile as young adults, which allowed us to generate individuals that were mutated for all three receptor genes. Remarkably, even these triple knockouts were viable, and several have been maintained in our colony for over one year.

Their viability notwithstanding, the triple mutants displayed multiple major organ defects, neurological abnormalities and physiological deficits. Altered histology, increased apoptosis and cellular degeneration, for example, were prominent in a variety of adult tissues, including the hippocampus, cerebellum and neocortex of the brain, the epithelium of the prostate, the parenchyma of the liver, and the walls of blood vessels. In addition, adult triple mutants were blind, owing to the postnatal degeneration of rods and cones in the retina (Q.L. and G.L., data not shown). The spleens of adult triple mutants were populated by apoptotic cells but were also grossly enlarged, with an average weight of 468 ± 79 mg ($n = 4$) compared to 93 ± 8 mg ($n = 3$) for wild type, consistent with aberrant homeostasis of the lymphoid populations in which expression of the three receptors is prominent[3,4,21], and with the demonstration that protein S is interleukin-4-inducible in T lymphocytes and is an inhibitor of cultured B- and T-cell proliferation[21]. These observations demonstrate that concerted activation of Tyro 3 family receptors is essential for the trophic maintenance and homeostatic balance of a wide variety of cell types in mature mammalian tissues.

Among the most severe phenotypes was that seen in the adult male gonads. Although the ovaries of triple-knockout females were histologically abnormal, with cell death evident in the granulosa cells associated with growing ovarian follicles (Q.L. and G.L., data not shown), several of these females were fertile. In contrast, triple

knockout males never sired offspring. The testes of adult triple mutants were one-third of the size of those of wild-type males, with an average weight of 35 ± 8 mg ($n = 6$), compared to 100 ± 5 mg ($n = 5$) for wild type; triple-mutant epididymi were invariably devoid of sperm. Spermatogenesis was clearly disrupted in the triple mutants, and the cellular organization of the seminiferous tubules was grossly perturbed (Fig. 2). These effects were first detectable only at three weeks after birth, approximately one week before the onset of sexual maturity, and embryonic and early neonatal development of the testes, including the generation of a full complement of normal testicular cell types, was not obviously affected. In young (4–8 weeks) adults, a reduced number of round spermatids was first noticeable at seminiferous tubule stages VII and VIII (refs 7, 22); many fewer spermatocytes at the pachytene stage of meiosis were also seen in these young males, and there were very few cells with the morphological features of mature sperm (Fig. 2a, b). The release of the few mature sperm that were produced was delayed beyond tubule stage VIII, the normal stage of release[22]. These deficiencies became progressively more severe as triple-mutant males aged (Fig. 2c, d); in 6-month old mice, we frequently observed tubules depleted of nearly all germ cells (Fig. 2e–h). Apoptotic cell death, detected by TUNEL staining, was markedly elevated in the young triple-mutant tubules (Fig. 2i, j), and was prominent in spermatids at tubule stages VII–VIII and in pachytene spermatocytes (the same points in spermatid and spermatocyte differentiation at which cell death is first observed following hypophysectomy and testosterone depletion[7,23,24]). Although apoptosis eventually depleted the testes of most germ cells, the proliferation of male stem cells (spermatogonia) continued for a time in young triple knockouts (Fig. 2k, l). Mutants carrying fewer receptor-gene mutations were also compromised with respect to spermatogenesis, although less severely. Tyro $3^{-/-}$Axl$^{+/+}$Mer$^{-/-}$ and Tyro $3^{-/-}$Axl$^{+/-}$Me$^{-/-}$ males had reduced testicular masses relative to wild type (52 and 43 mg, respectively), and only ~20% of Tyro $3^{-/-}$Axl$^{+/-}$Mer$^{-/-}$ males in our colony have sired offspring. These less-compromised mice also showed disordered spermatogenesis and reduced epididymal numbers of mature sperm. Less severe effects on fertility and testicular size, mass and histology were observed in Tyro $3^{-/-}$Axl$^{-/-}$Mer$^{+/+}$ males, and all single-mutant males appeared normal.
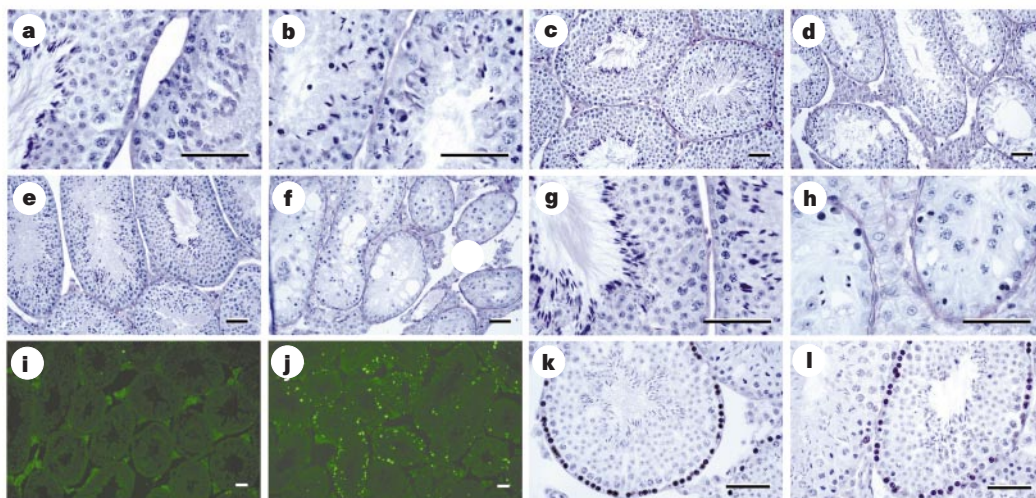
Figure 2 Aborted spermatogenesis and germ-cell death in seminiferous tubules of Tyro $3^{-/-}$Axl$^{-/-}$Mer$^{-/-}$ mice. **a**, **b**, Wild-type and triple-mutant seminiferous tubules, respectively, at 5 weeks after birth. The wild-type tubule section to the left of **a** is at late stage VII and contains many mature sperm. No mature sperm are evident in either of the two tubule sections in **b**, which contain stunted immature spermatids with improperly oriented acrosomes, and dying cells. **c**, **d**, Wild-type and triple-mutant tubules, respectively, at 18 weeks. Total cellularity of the triple-mutant tubules (**d**) is by this age substantially reduced. **e**, **f**, Wild-type and triple-mutant tubules, respectively, at 6 months. Some tubule sections (such as the central tubule in **f**) are entirely depleted of germ cells in the triple mutants. **g**, **h**, Wild-type and triple-mutant tubules, respectively, at 6 months. **i**, **j**, TUNEL staining for apoptotic cell-death in sections of wild-type and triple-mutant tubules, respectively, at 9 weeks; **i** contains a single TUNEL$^+$ cell; **j** contains 172 TUNEL$^+$ cells. **k**, **l**, Spermatogonial stem cell division, as measured by a 2-h pulse of BrdU, in wild-type and triple-mutant seminiferous tubules, respectively, at 5 weeks. All scale bars, 50 μm.
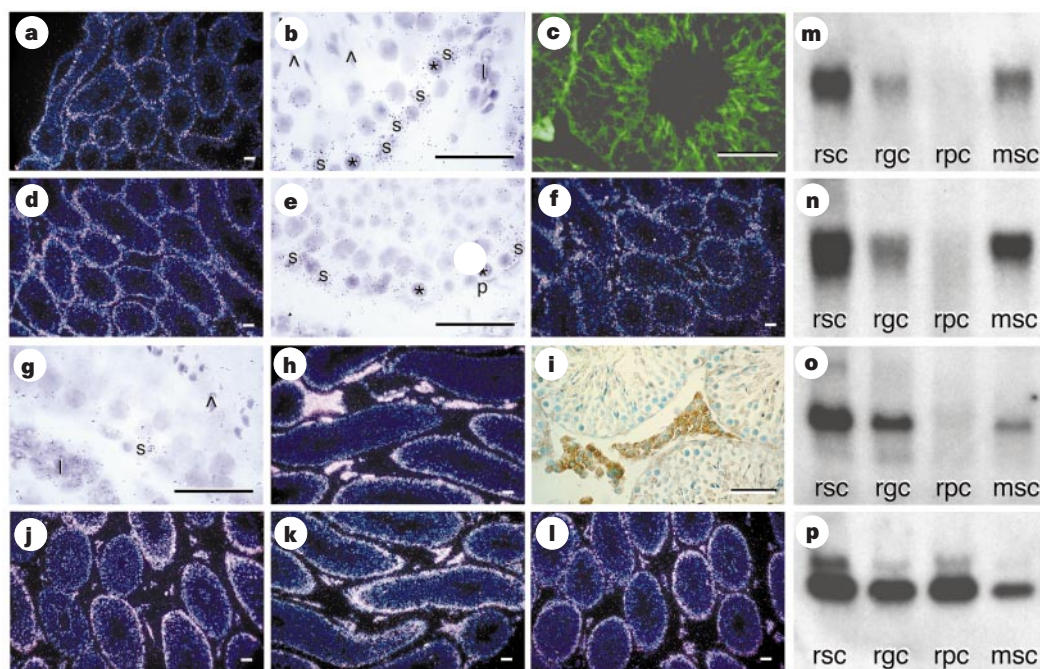
Figure 3 Tyro 3 family receptors and their ligands in the testes. **a**, *In situ* hybridization for Tyro 3 mRNA, expressed by cells at the periphery of all seminiferous tubule sections at 5 weeks. **b**, High-power, bright-field image of Tyro 3 mRNA (dark silver grains). Grains are located over lightly staining, irregularly shaped nuclei at the wall of the tubule, which are features of Sertoli-cell nuclei (s)[25], and not over the dark round nuclei of spermatogonia (asterisks), the Leydig cell nuclei outside the tubule (|), or spermatocyte or spermatid nuclei (∧). **c**, Immunolocalization of Tyro 3 protein[2] (green) on most Sertoli cell membrane surfaces. **d**, *In situ* hybridization for Axl mRNA, similar to the Tyro 3 profile in **a**. **e**, High-power, bright-field image of Axl mRNA localization, similar to the Tyro 3 profile in **b**. Note the absence of signal in peritubular cells (p). **f**, *In situ* hybridization for Mer mRNA, similar to the Tyro 3 profile in **a**. **g**, High-power, bright-field image of Mer mRNA localization. Note low signal in Leydig cells, not seen for Tyro 3 or Axl mRNA. **h**, *In situ* hybridization for Gas6 mRNA, highly expressed by Leydig cells, at 5 weeks. At this age, expression of Gas6 also first becomes detectable in a subset of Sertoli cells. **i**, Immunolocalization of Gas6 protein expression in Leydig cells at 4 weeks. **j**, *In situ* hybridization for Gas6 mRNA at 18 weeks. By this age, expression in Leydig and Sertoli cells is roughly equivalent, with a tubule-stage-specific regulation evident in the latter. (Sertoli cell expression is lowest at stages VII/VIII, the inverse of GATA-1 regulation.) **k**, *In situ* hybridization for protein S mRNA at 5 weeks, similar to the Gas6 profile in **h**. Although protein S mRNA is prominent in Leydig cells, it is also detected in Sertoli cells by this age. **l**, *In situ* hybridization for protein S mRNA at 18 weeks, similar to the Gas6 profile in **j**. **m–p**, Northern blots of total RNAs isolated from rat Sertoli cells (rsc), rat germ cells (rgc), rat peritubular cells (rpc), and mouse Sertoli cells (msc). Blots were hybridized with probes for Tyro 3 (**m**), Axl (**n**), SHBG, a marker for Sertoli cells (**o**), and cyclophilin as a loading/RNA control (**p**). All scale bars, 50 μm.

Although spermatids and spermatocytes are the cells most obviously affected by the loss of Tyro 3, Axl and Mer, these cells do not in fact express the three receptors (Fig. 3). Before and after sexual maturity, each of the receptor messenger RNAs was localized to the periphery of the seminiferous tubules (Fig. 3a, d, f). Of the three cell types with nuclei at this position (Sertoli cells, spermatogonia and peritubular cells) only Sertoli cells clearly expressed Tyro 3, Axl and Mer mRNAs. This assignment was based on: (1) the absence of an *in situ* hybridization signal in the thin peritubular cells that surround the tubule (Fig. 3b, e, g); (2) the patchy circumferential distribution of receptor *in situ* signals and their association with the lightly staining, irregularly shaped nuclei characteristic of Sertoli cells[25], as opposed to the darkly staining, round nuclei of spermatogonia (Fig. 3a–g); (3) the presence of receptor mRNAs in cells that express sex-hormone-binding globulin, a Sertoli cell marker[5] (Fig. 3m–o); and (4) the distribution of northern blot signals in RNAs isolated from enriched populations of testicular cells (Fig. 3m–o). In addition, antibodies raised against Tyro 3 (ref. 2) specifically stained Sertoli cells, which are large secretory cells whose cytoplasm extends across the full radial extent of the tubule[25] (Fig. 3c). Together, these data demonstrate that Tyro 3, Axl and Mer are Sertoli-cell products, although low-level expression by spermatogonia cannot be definitively excluded. Sertoli-cell expression of the receptor mRNAs was observed throughout postnatal development, with a modest peak at five weeks after birth (Fig. 3a, d, f). At all times, the amount of mRNA was greatest for Tyro 3 and Axl, and less for Mer. Unlike Tyro 3 and Axl mRNAs, a low level of Mer mRNA was also detected in the testosterone-producing Leydig cells that lie outside the tubules (Fig. 3g).

In contrast to the receptors, their ligands were each expressed during the first three postnatal weeks by Leydig cells (Fig. 3h–l). There was a pronounced spike in Leydig cell Gas6 at the onset of sexual maturity (Fig. 3h, i); this expression declined and stabilized in mature adults (Fig. 3j). Co-incident with sexual maturation, Gas6 mRNA and protein also appeared in Sertoli cells (Fig. 3h). This Sertoli-cell signal was first detected at stage IX during the first wave of spermatogenesis to pass through the tubule, and became increasingly prominent with postnatal age, such that in mature testes roughly comparable levels of Gas6 were detected in Leydig and Sertoli cells (Fig. 3j). Sertoli-cell expression of Gas6 in the mature testes exhibited a distinctive rising-and-falling regulation as a function of tubule stage; preliminary analysis indicates that expression is highest at stages III–IV and is almost undetectable by stage VIII (Fig. 3j). This periodic cycling with tubule stage is a property exhibited by many other Sertoli-cell gene products, including the transcription factor GATA-1 (ref. 26) (see below). Protein S shows a similar development profile (Fig. 3k, l), although its overall expression was less than that of Gas6, and Sertoli cells became protein-S-positive about one week before they became Gas6-positive. Protein S levels also fluctuated with tubule stage, although the amplitude of this fluctuation was smaller than for Gas6. Thus, ligand–receptor signalling for the Tyro 3 family in the testes switches from a paracrine to an autocrine/paracrine mode at the onset of sexual maturity.
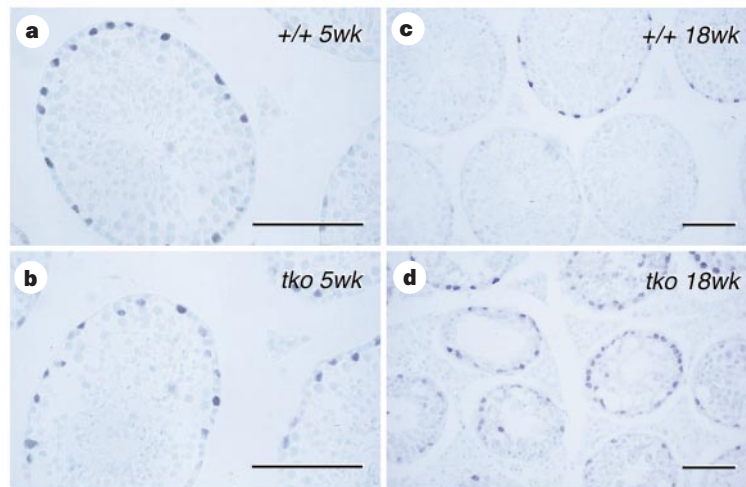
Figure 4 Expression of GATA-1 in wild-type (+/+) and triple-mutant (tko) testes. **a**, **b**, GATA-1 immunoreactive (dark blue) nuclei in sections of wild-type and triple-mutant seminiferous tubules, respectively, at 5 weeks. GATA-1$^+$ Sertoli cells are present in the triple mutant at this age. **c**, **d**, GATA-1 immunoreactivity at 18 weeks. GATA-1 expression persists in tubule sections of the triple mutant (**d**), and in contrast to wild-type (**c**), this expression is evident in nearly all tubules, independent of tubule stage. All scale bars, 100 μm.

These observations indicated that germ-cell death in the triple mutants might result from the death of Sertoli cells. This is not the case: we readily detected GATA-1$^+$ Sertoli cells within the tubules of young adult triple knockouts (Fig. 4a, b), and the number of GATA-1$^+$ cells significantly increased in more mature triple mutants relative to wild-type (Fig. 4c, d). Sertoli-cell expression of GATA-1 also fluctuates with tubule stage in the mature testes, with a peak at tubule stages VII/VIII (Fig. 3c)[26], and germ cells inhibit GATA-1 expression at other tubule stages[26]. We found that, in the germ-cell-depleted tubules of older mutants, most Sertoli cells express GATA-1 independently of tubule stage (Fig. 4d).

Sertoli cells provide essential physical and trophic support for developing spermatogonia, spermatocytes and spermatids. This tropic support in turn depends on a network of reciprocal signalling interactions between Leydig cells, Sertoli cells, peritubular cells and germ cells within the testes[5], and on upstream hormonal regulation from the pituitary. Although intratesticular interactions are well understood at a cellular level, the underlying signalling molecules have, with the exception of testosterone itself, remained elusive. Our results now identify the Tyro 3 family receptors and their ligands as essential regulators of Sertoli-cell function. The fact that the *Tyro 3*, *Axl* and *Mer* genes must all be disrupted for maximal germ-cell degeneration to occur indicates that these receptors act additively or in combination; their combined activation in Sertoli cells may be required for the production of the germ-cell trophins that these cells must produce. Although the spermatotoxic effects seen in the triple knockouts are in many respects similar to those following hypophysectomy or testosterone deprivation[23,24], other behavioural and physiological effects of these manipulations are not evident in the mutants: these mice exhibit normal sexual behaviour, have histologically intact seminal vesicles, and have circulating testosterone levels in the normal range – 75, 85 and 185 ng dl^{-1} for three triple knockout males at 3 months compared to 48, 105 and 110 ng dl^{-1} for three wild-type males of the same age.

As (1) Gas 6 and protein S are related in sequence and predicted structure to sex-hormone-binding globulin; (2) the primary cellular target of testosterone in the seminiferous tubule is the Sertoli cell; (3) Leydig cells produce both testosterone and Gas6/protein S; and (4) abrogation of signalling through Tyro 3 family receptors leads to germ-cell effects similar to those of testosterone depletion, we suggest that the actual ligands for Tyro 3 family receptors may be hybrid molecules of Gas6 or protein S bound to testosterone or (in other cells) other steroids. Given the large and controversial literature on cell-surface, non-genomic effects of steroids, we are currently investigating this possibility. □

Methods

Gene inactivation. Each of the receptor genes was disrupted using a G418 (neomycin)-resistance cassette, and the inactivated genes were used to replace their normal counterparts by homologous recombination in mouse embryonic stem (ES) cells (Fig. 1). A *Kpn*I–*Bam*HI (K–B) fragment containing exon 9 and a portion of exon 10 of the *Tyro 3* gene (striped bar in Fig. 1a) was replaced with the resistance cassette (neo), used for positive selection in ES cells[19]. A thymidine-kinase cassette (tk) was used to select against non-homologous recombinants. An *Xba*I–*Hin*dIII fragment containing exon 9 of the *Axl* gene (striped bar in Fig. 1d), and a 3.1-kb *Bam*HI–*Spe*I fragment of the *Mer* gene (striped bar in Fig. 1g) were both similarly replaced, and tk was in each case used for negative selection. ES cells heterozygous for the inactivated genes were injected into wild-type mouse blastocysts to generate chimaeras, which were then bred and intercrossed in subsequent generations to yield mice homozygous for each of the mutations, according to standard protocols[19]. Loss of functional Tyro 3, Axl or Mer in these mice was confirmed by western and/or RNA analysis (Fig. 1c, f, i; and data not shown). The primers used for the RT-PCR experiments of Fig. 1i were from nucleotides 1,963–1,984 (>, forward) and 2,736–2,757 (<, reverse) of the mouse Mer cDNA (ref. 4).

Expression studies. Gas6 and GATA-1 antibodies were purchased from Santa Cruz Biologicals. *In situ* hybridization, western blots, northern blots, and immunohistochemistry were performed as described[2,8,14]. ^{33}P-riboprobes were used for *in situ* hybridizations, antibody binding to westerns was detected by ECL chemiluminescence, and northerns were hybridized with ^{32}P-radiolabelled DNA probes. Seminiferous tubule-cell populations were separated by standard protocols[5–7]. Isolation methods result in highly purified populations of Sertoli and peritubular cells, but germ-cell preparations contain some Sertoli cells, as shown by the distribution of sex-hormone-binding globulin signal (Fig. 3p). Exposure times for *in situ* hybridizations of Fig. 3: j, 12 days; z, b, d, e, h, k, l, 15 days; f, g, 21 days.

1. Crosier, K. E. & Crosier, P. S. New insights into the control of cell growth; the role of the Axl family. *Pathology* **29**, 131–135 (1997).
2. Lai, C., Gore, M. & Lemke, G. Structure, expression, and activity of Tyro 3, a neural adhesion-related receptor tyrosine kinase. *Oncogene* **9**, 2567–2578 (1994).
3. O'Bryan, J. P. *et al.* Axl, a transforming gene isolated from primary human myeloid leukemia cells, encodes a novel receptor tyrosine kinase. *Mol. Cell. Biol.* **11**, 5016–5031 (1991).
4. Graham, D. K., Dawson, T. L., Mullaney, D. L., Snodgrass, H. R. & Earp, H. S. Cloning and mRNA expression analysis of a novel human protooncogene, c-mer. *Cell Growth Differ.* **5**, 647–657 (1994).
5. Skinner, M. K. Cell-cell interactions in the testis. *Endocrine Rev.* **12**, 45–77 (1991).
6. Skinner, M. K. in *The Sertoli Cell* (eds Russell, L. D. & Griswold, M. D.) 237–247 (Cache River, Clearwater, Florida, 1993).

7. Griswold, M. D. Interactions between germ cells and Sertoli cells in the testis. *Biol. Reprod.* **52**, 211–216 (1995).
8. Lai, C. & Lemke, G. An extended family of protein-tyrosine kinase genes differentially expressed in the vertebrate nervous system. *Neuron* **6**, 691–704 (1991).
9. Mark, M. R. *et al.* RSE, a novel receptor-type tyrosine kinase with homology to Axl/Ufo, is expressed at high levels in the brain. *J. Biol. Chem.* **269**, 10720–10728 (1994).
10. Taylor, I. C., Roy, S., Yaswen, P., Stampfer, M. R. & Varmus, H. E. Mouse mammary tumors express elevated levels of RNA encoding the murine homology of SKY, a putative receptor tyrosine kinase. *J. Biol. Chem.* **270**, 6872–6880 (1995).
11. Rescigno, J., Mansukhani, A. & Basilico, C. A putative receptor tyrosine kinase with unique structural topology. *Oncogene* **6**, 1909–1913 (1991).
12. Janssen, J. W. *et al.* A novel putative tyrosine kinase receptor with oncogenic potential. *Oncogene* **6**, 2113–2120 (1991).
13. Jia, R. & Hanafusa, H. The proto-oncogene of v-eyk (v-ryk) is a novel receptor-type protein tyrosine kianse with extracellular Ig/GN-III domains. *J. Biol. chem.* **269**, 1839–1844 (1994).
14. Stitt, T. N. *et al.* The anticoagulation factor protein S and its relative, Gas6, are ligands for the Tyro 3/Axl family of receptor tyrosine kinases. *Cell* **80**, 661–670 (1995).
15. Godowski, P. J. *et al.* Reevaluation of the roles of protein S and Gas6 as ligands for the receptor tyrosine kinase Rse/Tyro 3. *Cell* **82**, 355–358 (1995).
16. Chen, J., Carey, K. & Godowski, P. J. Identification of Gas6 as a ligand for Mer, a neural cell adhesion molecule related receptor tyrosine kinase implicated in cellular transformation. *Oncogene* **14**, 2033–2039 (1997).
17. Nagata, K. *et al.* Identification of the product of growth arrest-specific gene 6 as a common ligand for Axl, Sky, and Mer receptor tyrosine kinases. *J. Biol. Chem.* **271**, 30022–30027 (1996).
18. Joseph, D. R. Sequence and functional relationships between androgen-binding protein/sex hormone-binding globulin and its homologs protein S, Gas6, laminin, and agrin. *Steroids* **62**, 578–588 (1997).
19. Capecchi, M. R. Altering the genome by homologous recombination. *Science* **244**, 1288–1292 (1989).
20. Camenisch, T. D., Koller, B. H., Earp, H. S. & Matsushima, G. K. A novel receptor tyrosine kinase, Mer, inhibits TNF-α production and lipopolysaccaride-induced endotoxic shock. *J. Immunol.* **162**, 3498–3503 (1999).
21. Smiley, S. T., Stitt, T. N. & Grusby, M. J. Cross-linking of protein S bound to lymphocytes promotes aggregation and inhibits proliferation. *Cell. Immunol.* **181**, 120–126 (1997).
22. Leblond, C. P. & Clemont, Y. Definition of the stages of the cycle of the seminiferous epithelium in the rat. *Ann. N. Y. Acad. Sci.* **55**, 548–573 (1952).
23. Henriksén, K., Hakovirta, H. & Parvinen, M. Testosterone inhibits and induces apoptosis in rat seminiferous tubules in a stage-specific manner. *Endocrinology* **136**, 3285–3291 (1995).
24. Sun, Y.-T, Wreford, N. G., Robertson, D. M. & De Kretser, D. M. Quantitative cytological studies of spermatogenesis in intact and hypophysectomized rats: Identification of androgen-dependent stages. *Endocrinology* **127**, 1215–1223 (1991).
25. Wong, V. & Russell, L. D. Three-dimensional reconstruction of a rat stage V Sertoli cell: I. Methods, basic configuration, and dimensions. *Am. J. Anat.* **167**, 143–161 (1983).
26. Yomogida, K. *et al*. Developmental stage- and spermatogenic cycle-specific expression of transcription factor GATA-1 in mouse Sertoli cells. *Development* **120**, 1759–1766 (1994).
27. Lewis, P. A., Crosier, K. E., Wood, C. R. & Crosier, P. S. Analysis of the murine Dtk gene identifies conservation of genomic structure within a new receptor tyrosine kinase subfamily. *Genomics* **31**, 13–19 (1996).
28. Biesecker, L. G., Giannola, D. M. & Emerson, S. G. Identification of alternative exons, including a novel exon, in the tyrosine kinase receptor gene Etk2/tyro3 that explains differences in 5′ cDNA sequences. *Oncogene* **10**, 2239–2242 (1995).
29. Schulz, A. S., Schleithoff, L., Faust, M., Bartram, C. R. & Janssen, J. W. G. The genomic structure of the human UFO receptor. *Oncogene* **8**, 509–513 (1993).
30. Bellosta, P., Zhang, Q., Goff, S. P. & Basilico, C. Signaling through the ARK tyrosine kinase receptor protects from apoptosis in the absence of growth stimulation. *Oncogene* **15**, 2387–2397 (1997).

Binding of double-strand breaks in DNA by human Rad52 protein

Eric Van Dyck*, Alicja Z. Stasiak†, Andrzej Stasiak† & Stephen C. West*

* *Imperial Cancer Research Fund, Clare Hall Laboratories, South Mimms, Herts EN6 3LD, UK*

† *Laboratoire d'Analyse Ultrastructurale, Université de Lausanne, CH-1015 Lausanne-Dorigny, Switzerland*

....

Double-strand breaks (DSBs) in DNA are caused by ionizing radiation. These chromosomal breaks can kill the cell unless repaired efficiently, and inefficient or inappropriate repair can lead to mutation, gene translocation and cancer[1]. Two proteins that participate in the repair of DSBs are Rad52 and Ku: in lower eukaryotes such as yeast, DSBs are repaired by Rad52-dependent homologous recombination, whereas vertebrates repair DSBs
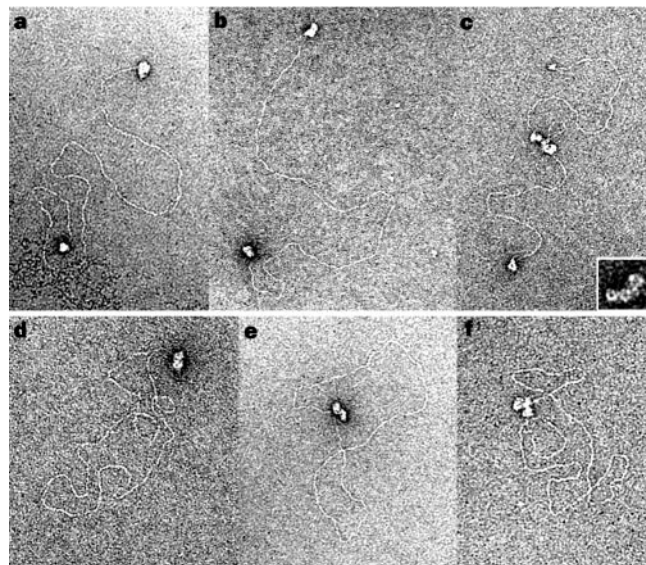
Figure 1 DNA end-binding and end-to-end interactions promoted by hRad52. Complexes formed between hRad52 and linear duplex DNA containing single-stranded tails were visualized by electron microscopy. **a**, **b** and **f**, 3′ single-stranded (ss) DNA tails. **c**, **d** and **e**, 5′ ssDNA tails. Inset in **c** shows a close-up view of an end-binding complex in which hRad52 rings are evident. Reactions (20 µl) contained 10 µM (**a**, **d**) or 4.7 µM (**b**, **c**, **e**, **f**) tailed duplex DNA in 20 mM triethanolamine-HCl (pH 7.5). After 5 min at 37 °C, hRad52 was added to 0.16 µM (**a**, **d**) or 0.08 µM (**b**, **c**, **e**, **f**) and incubation was continued for 15 min.

primarily by Ku-dependent non-homologous end-joining[2]. The contribution of homologous recombination to vertebrate DSB repair, however, is important[3,4]. Biochemical studies indicate that Ku binds to DNA ends and facilitates end-joining[5]. Here we show that human Rad52, like Ku, binds directly to DSBs, protects them from exonuclease attack and facilitates end-to-end interactions. A model for repair is proposed in which either Ku or Rad52 binds the DSB. Ku directs DSBs into the non-homologous end-joining repair pathway, whereas Rad52 initiates repair by homologous recombination. Ku and Rad52, therefore, direct entry into alternative pathways for the repair of DNA breaks.

In lower eukaryotes, double-strand breaks in meiotic and mitotic cells are processed to form single-stranded tails, in reactions that involve the Mre11/Rad50/Xrs2 protein complex[6,7]. Similar processing events are thought to occur in higher cells, where homologues of Mre11, Rad50 and Xrs2 (p95) exist[2]. In yeast *rad52* mutants, exonuclease degradation is more extensive than in wild-type cells[7], indicating that the Rad52 protein may be involved in the protection or processing of the initial DSB. We therefore tested whether Rad52 acts at the early stages of double-strand-break repair by direct interaction with the DSB or partially resected DSB. Complexes were formed between human Rad52 protein (hRad52) and linear duplex DNA, and were visualized by electron microscopy. Using substrates containing 5′ or 3′ single-stranded tails (approximately 300 nucleotides in length), we observed that hRad52 bound preferentially to the ends of the DNA (Fig. 1). Molecules in which both ends of the linear DNA were bound by hRad52 are shown in Fig. 1a–c.

We found that a large percentage of the linear DNA (~90%) present on each grid was held together by hRad52-mediated intermolecular interactions. Indeed, end-to-end associations between DNA molecules, mediated by hRad52, resulted in the formation of large DNA–protein networks (data not shown). However, away from the networks, isolated DNA molecules were observed in which Rad52 protein clearly provided an intramolecular bridge between two ends, resulting in their recircularization (Fig. 1d–f). When 46